Optimized and transferable nonlocal separable *ab initio* pseudopotentials

J. S. Lin,* A. Qteish,† M. C. Payne, and V. Heine
Cavendish Laboratory, Madingley Road, Cambridge CB3 OHE, United Kingdom
(Received 4 March 1992; revised manuscript received 27 August 1992)

The purpose of the present work is to obtain a better atomic pseudopotential with respect to convergence and computational efficiency while retaining reasonable transferability in the context of electronic-structure calculations for solids using a plane-wave basis set. We introduce a systematic procedure for generating optimized nonlocal pseudopotentials by minimizing the high Fourier components of the pseudo-wave-functions with the constraints of normalization and continuity of first and second derivatives of the wave function at the core radius. This is based on the recent ideas of Rappe *et al.* (RRKJ) [Phys. Rev. B **41**, 1227 (1990)], but overcomes certain difficulties which we have found with the RRKJ scheme. For computational efficiency this optimized nonlocal pseudopotential is transformed into a Kleinman-Bylander (KB) form. To ensure the transferability we first compare the logarithmic derivative of the all-electron wave function with that of the final KB form of the optimized nonlocal pseudopotential over a wide range of energies. We then test the KB form of the potential in a number of atomic environments. The structural properties of ZnS are calculated to demonstrate the reliability of our optimized nonlocal separable *ab initio* pseudopotential and its total-energy convergence.

I. INTRODUCTION

The theoretical study of solid-state materials using electronic-structure calculations is currently an extremely active field of research in solid-state physics. One of the most popular methods is within the local-density approximation of density-functional theory[1] using the pseudopotential approximation and plane-wave basis sets.[2] In particular, with the development of the Car-Parrinello molecular-dynamics scheme[3] and conjugate gradient methods,[4] it has become possible to study very large systems. But, even with modern computer technology, the application of this method to some more problematic materials, such as those containing first-row elements or transition metals, is still very difficult due to the fact that an enormous number of plane waves are needed to represent the sharply peaked valence states arising from the strongly attractive pseudopotentials. Furthermore, the pseudopotentials of these elements are strongly nonlocal, and handling the nonlocality can result in computational inefficiency in the electronic-structure calculations.[5] Therefore the possibility of generating much smoother and more efficacious forms of nonlocal pseudopotentials for a wide range of applications has attracted much interest recently.[6,7]

By following a method for producing optimized norm-conserving pseudopotentials introduced by Rappe, Rabe, Kaxiras, and Joannopoulos (RRKJ),[8] some improvement in the convergence of pseudopotential total-energy calculations with respect to plane-wave cutoff can be easily achieved. This immediately led us to try to generate optimized nonlocal pseudopotentials of RRKJ-type and transform them to Kleinman-Bylander (KB) (Ref. 5) form in order to improve both convergence and computational efficiency. However, we experienced technical difficulties when we tried to use the RRKJ scheme, and these in turn prevented us from constructing smoother nonlocal pseudopotentials in KB form. Also, it was realized that much wider tests of the transferability of the KB form of the optimized nonlocal pseudopotential are necessary to allow its use in different solid environments. In fact, generating a good pseudopotential has been a bit of a black art.

In this work, we improve the RRKJ scheme and develop a much more systematic procedure to generate an optimized and smooth nonlocal pseudopotential. The potential is then transformed into KB form, and its transferability is tested. In Sec. II, we briefly review the optimized pseudopotential scheme of RRKJ, describe the technical problems we met when using this scheme, and show how we overcame them to achieve both convergence and smoothness. The resulting potential turns out to converge much better than a recent "smooth" pseudopotential of Troullier and Martins.[6] In Sec. III, we review the KB form of nonlocal pseudopotentials, and then we discuss testing the transferability of our optimized nonlocal pseudopotentials in KB form. Finally, in Sec. IV, the structural properties of ZnS are investigated to demonstrate the success of our optimized and transferable nonlocal separable *ab initio* pseudopotential and its total-energy convergence.

II. OPTIMIZING PSEUDOPOTENTIALS FOR CONVERGENCE AND SMOOTHNESS

Recently RRKJ proposed that the convergence of the total energy of a solid with the cutoff energy for the plane-wave basis set mirrors the convergence of the total energies of the isolated pseudoatoms which comprise the solid. Also, by using scaling arguments they proved that total-energy convergence and kinetic-energy convergence are very similar in the limit of large cutoff energies. These two statements led them to design a scheme in which the kinetic energy in the high Fourier components of the pseudo-wave-functions is minimized to achieve optimal convergence.

 ©1993 The American Physical Society

A brief description of the RRKJ scheme is as follows. First, the pseudo-wave-function $\Psi_l(r)$ inside core radius (r_c) is expressed as

$$\Psi_l(r)=\sum_{i=1}^{n}\alpha_i j_l(q_i r) \quad \text{with} \quad \frac{j_l'(q_i r_c)}{j_l(q_i r_c)}=\frac{\phi_l'(r_c)}{\phi_l(r_c)} , \tag{2.1}$$

in which the $j_l(q_i r)$ are spherical Bessel functions with $(i-1)$ zeros less than r_c, and $\phi_l(r)$ is the all-electron wave function. Second, Lagrange multipliers are used to constrain the normalization and the continuity of the first two derivatives of the wave function at r_c, and the coefficients α_i are determined by minimizing the kinetic energy beyond the cutoff q_c, which can be expressed as

$$\Delta E_k(\alpha_1,\alpha_2,\ldots,\alpha_n,q_c) = -\int_0^{\infty} d^3\mathbf{r}\,\Psi_l^*(\mathbf{r})\nabla^2\Psi_l(\mathbf{r})-\int_0^{q_c} d^3\mathbf{q}\,\mathbf{q}^2|\Psi_l(\mathbf{q})|^2 . \tag{2.2}$$

Here $\Psi_l(\mathbf{q})$ is the Fourier transform of $\Psi_l(\mathbf{r})$. Third, the optimized pseudopotential $V_l(r)$ is then constructed by directly inverting the radial Kohn-Sham equation with the optimized pseudo-wave-function $\Psi_l(\mathbf{r})$ in order to generate the pseudopotential operator $V_{\rm SL}(\mathbf{r})$ in the usual so-called "semilocal" form

$$V_{\rm SL}(\mathbf{r})=\sum_l V_l(r)\mathcal{P}_l = V_{\rm loc}(r)+\sum_l \Delta V_l(r)\mathcal{P}_l , \tag{2.3}$$

$$\Delta V_l(r)=V_l(r)-V_{\rm loc}(r) \quad \text{for } r<r_c , \tag{2.4}$$

where $\mathcal{P}_l$ is a projection operator onto angular momentum l and $V_{\rm loc}$ is a local potential which is chosen arbitrarily. We use atomic units $e=\hbar=m=1$ except that energies are given in Rydbergs (Ry).

From a practical point of view, what matters is how to choose the three parameters r_c, q_c, and n. RRKJ proposed the following procedure which we shall refer to as "the RRKJ scheme":

(i) The r_c should be chosen to ensure transferability.

(ii) For n, they suggested using ten or even more spherical Bessel functions.

(iii) The q_c is determined iteratively by reducing the convergence error ΔE_k in the kinetic energy to just below some prechosen tolerance.

We have found some practical problems with all stages of this procedure. First, the minimization of ΔE_k in (2.2) can be very difficult to perform if there are q_i's included in (2.1) which are much larger than q_c. In such a case, we find the resulting optimized pseudopotential has strong short-wavelength oscillations. This problem has also been pointed out by Troulier and Martins.[6] However, one has to have n large enough to give a good pseudopotential which is accurate over a reasonable energy range. Second, from the point of view of transferability there is often an advantage in having r_c as small as possible, but we have found there is very little gain from the optimization procedure if r_c is chosen too small. Moreover, we have used a simple method of testing the transferability of the pseudopotential by mimicking changes in solid-state environment by changes in atomic configuration. We shall illustrate each of these points with the numerical example presented below. By showing how these three parameters r_c, q_c, and n interact, we shall demonstrate how to change the process of determining of optimized pseudopotential from a somewhat black art to a more rational procedure, at least as far as the optimized generation is concerned.

We now take Zn as an example to demonstrate the technical problems we described above. Due to the lack of inner core d states, Zn represents one of the most difficult transition metals to converge with respect to the cutoff energy for the plane-wave basis set in a pseudopotential total-energy calculation. However, only the $3d$ eigenstate has to be optimized to improve the convergence. The Zn valence neutral state with configuration $3d^{10}4s^{1.73}4p^{0.27}$ has been used to generate $3d$ pseudopotentials with core radii of 2.0 and 1.50 bohr. By matching of the logarithmic derivative of the spherical Bessel functions with that of the all-electron wave function at the two different values of r_c, the wave vectors q_i have been determined and these values are shown in Table I. From Table I it is clear that the larger the value of r_c, the smaller the wave vectors q_i. Now we generate the optimized pseudo-wave-function based on the RRKJ scheme, except that the q_c is chosen as q_4, and transform this optimized pseudo-wave-function into Fourier space. Figure 1 shows the high Fourier components of the optimized pseudo-wave-function of the RRKJ scheme with $n=10$, and compares it with an unoptimized pseudo-wave-function generated with the Kerker scheme.[9] As expected, RRKJ optimization more or less cuts out the high Fourier components with $q>7$. However, a small oscillating tail remains. The effect of the latter is much more apparent in the pseudopotential shown in Fig. 2, where sharp oscillations also are seen at $r<r_c$.

We have seen that taking n too large results in unnecessary short-wavelength oscillations in the pseudopotential and actually detracts somewhat from the smoothness. On the other hand, we have to choose n large enough in order to give a good pseudopotential that is

TABLE I. The first ten wave vectors (q_i's) of the spherical Bessel functions of angular momentum 2 determined by fitting the logarithmic derivative to that of $3d$ all-electron wave function (2.1) at core radii of 2.00 and 1.50 bohr, respectively.

q_i $(\text{Ry})^{1/2}$	$r_c=2.00$ (bohr)	$r_c=1.50$ (bohr)
q_1	2.236 36	2.935 70
q_2	3.842 30	5.140 64
q_3	5.422 46	7.287 45
q_4	6.994 43	9.416 79
q_5	8.562 75	11.538 43
q_6	10.129 12	13.655 98
q_7	11.694 31	15.771 11
q_8	13.258 75	17.884 67
q_9	14.822 68	19.997 16
q_{10}	16.386 24	22.108 89

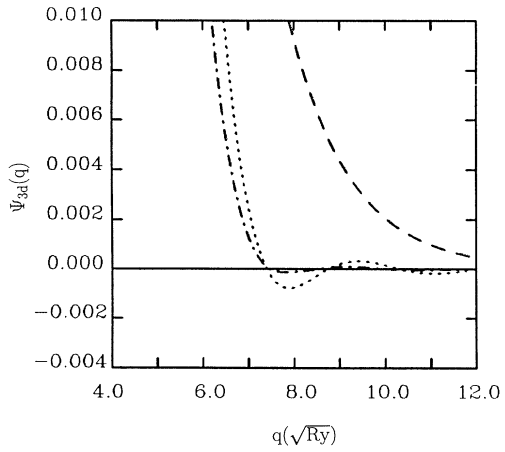

FIG. 1. Kerker pseudo-wave-function (dashed line), optimized pseudo-wave-function with $n=4$ and $q_c=q_4$ (dash-dotted line), and optimized pseudo-wave-function with $n=10$ and $q_c=q_4$ (dotted line) in Fourier space for the Zn $3d$ eigenstate with a core radius of 2.00 bohr.

transferable, i.e., valid over a wide range of energies. What matters here is that the pseudopotential has the right shape to give a good logarithmic derivative, not only at the atomic eigenvalue used to generate the pseudopotential but over a reasonable range of energy. To solve this conflict, we first investigate how many constraints are needed to generate our pseudopotential. Due to the fitting of the logarithmic derivative of the spherical Bessel functions with that of the all-electron wave function at r_c, we need three constraints, i.e., normalization and continuity of the first two derivatives of the wave function at r_c, to generate the norm-conserving pseudopotential. After adding the fourth requirement of minimizing the kinetic energy beyond q_c in Fourier space in (2.2), we need at least four spherical Bessel functions, and hopefully this will be enough to generate a good optimized pseudopotential. At the same time, it is easy to show that the smoothness can become worse by increasing n, which introduces unwanted oscillations as already discussed. Furthermore, the q_c cannot be reduced arbitrarily as envisaged in the RRKJ scheme, because it is essentially determined by the highest Fourier component in the pseudo-wave-function, effectively by the highest q_i which is q_4 for four spherical Bessel functions. We then expect good convergence with an energy cutoff at q_4^2 Ry. Thus we predict from Table I that total-energy calculations for Zn using $3d$ optimized pseudopotentials with core radii of 2.00 and 1.5 bohr should converge around 50 and 90 Ry, respectively, as was indeed found in the calculation on ZnS in Sec. IV. These results also demonstrate that there is a limit to what can be gained from the optimization scheme if r_c is chosen too small.

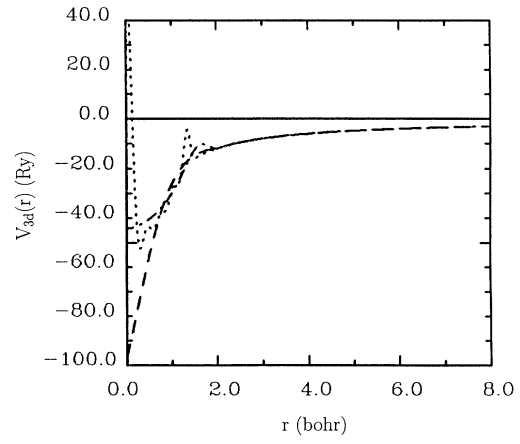

FIG. 2. Kerker pseudopotential (dashed line), optimized pseudopotential with $n=4$ and $q_c=q_4$ (dash-dotted line), and optimized pseudopotential with $n=10$ and $q_c=q_4$ (dotted line) generated for the Zn $3d$ eigenstate. The core radius is 2.00 bohr.

Following the above considerations, we can now present our modified scheme for generating an optimized pseudopotential, which we believe is more systematic than the RRKJ scheme. Moreover, the optimized pseudopotential is much smoother. We use the same equations and steps in (2.1) to (2.4): the difference lies in the practicalities of how we use them and set r_c, n, and q_c. We replace (i), (ii), and (iii) above in the RRKJ scheme by the following scheme.

(a) The r_c is set as large as possible, consistent with satisfactory transferability of the pseudopotential. What constitutes "satisfactory" depends on the physical system in question: it is a complicated question that arises in any use of pseudopotentials, but has nothing to do directly with optimization of the potential. However, one can use changes of atomic configuration to mimic changes in solid-state environment and hence to test transferability.

(b) We set $n=4$ to avoid any tail of high-energy Fourier components.

(c) We set $q_c=q_4$ because the energy cutoff is really controlled by q_4 and cannot be varied at will.

We want to emphasize that our scheme is now similar in its practical application to the scheme of Kerker[9] and Hamann, Schlüter, and Chang (HSC),[10] and certainly it is no more difficult to implement. The point is that we have four equations to solve for the four constants α_i in (2.1) in order to satisfy the three constraints on the wave function (the first two derivatives at r_c and normalization) plus the minimization of (2.2).

Using our new procedure we have generated the $3d$ nonrelativistic optimized pseudo-wave-function of Zn in the same non-spin-polarized valence-state configuration as above with an r_c of 2.0 bohr. For comparison, we have also constructed the $3d$ nonrelativistic pseudo-wave-function of Zn using the Kerker scheme[9] with the same configuration. As can be seen very easily from Fig. 3, the maximum of our optimized pseudo-wave-function moves substantially outwards with respect to that of the all-electron wave function and the Kerker pseudo-wave-function. The effect of this displacement on the transferability of the KB form of the nonlocal pseudopotential turned out to be very small, as was indeed found in the test of transferability in Sec. III. The Fourier components of the resulting pseudo-wave-functions are shown in Fig. 1. As expected, the kinetic energy con-

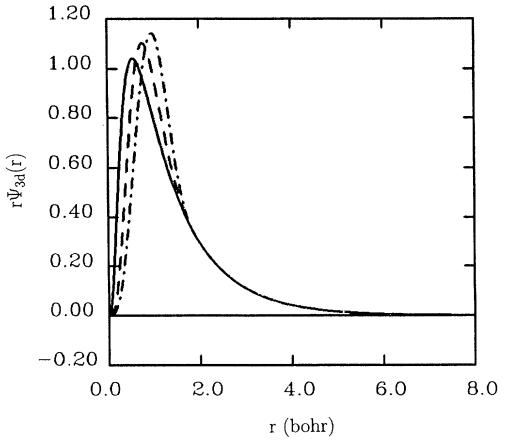

FIG. 3. All-electron wave function (solid line), Kerker pseudo-wave-function (dashed line), and optimized pseudo-wave-function (dash-dotted line) in real space for the Zn 3*d* eigenstate. The core radius is 2.00 bohr.

verged at roughly $q_4^2=50$ Ry for our optimized pseudo-wave-function, in contrast to 140 Ry for the Kerker one. The corresponding pseudopotential shown in Fig. 2 is also much smoother and shallower than the RRKJ and Kerker ones, which presumably accounts for the better convergence and smoothness.

Incidentally, Fig. 2 shows that our optimized pseudopotential (dash-dot curve) has a small wiggle in real space at $r\approx 1.8$ bohr. This is introduced by the optimization process, and can be understood as follows in terms of what is sometimes called the Gibbs phenomenon. If we have a Fourier series for, say, a repeated rectangular step function, and truncate the Fourier series at a finite point, then the corresponding real function has sprouted some overshoot wiggles near the sharp edge. They result from setting all Fourier components equal to zero beyond the cutoff. Of course the wiggles introduce some high Fourier components, but their amplitude and sign are such as to cancel the high Fourier components from the rest of the function, or in our case from the rest of the pseudopotential.

III. KLEINMAN-BYLANDER POTENTIALS AND THEIR TRANSFERABILITY

For computational efficiency, when performing pseudopotential total-energy calculations with plane waves, the semilocal form (2.3) of the pseudopotential operator $V_{\rm SL}(r)$ is usually transformed into the separable nonlocal form suggested by Kleinman and Bylander,[5]

$$V_{\rm KB}(r)=V_{\rm loc}(r)+\frac{|\Delta V_l(r)\Psi_l(r)\rangle\langle\Psi_l(r)\Delta V_l(r)|}{\langle\Psi_l(r)|\Delta V_l(r)|\Psi_l(r)\rangle}\mathcal{P}_l\ , \tag{3.1}$$

$$\Delta V_l(r)=V_l(r)-V_{\rm loc}(r)\quad \text{for } r<r_c\ . \tag{3.2}$$

Here $V_l(r)$ is constructed by directly inverting the radial part of the pseudo-wave-function $\Psi_l(r)$ to generate the semilocal form of the pseudopotential operator $V_{\rm SL}(r)$ in (2.3), and $V_{\rm loc}(r)$ is a local potential which again is chosen arbitrarily.

When we tried to transform the optimized pseudopotential generated with the RRKJ scheme into the KB form (3.1), we found problems of numerical instabilities. We traced the problem to the short-wavelength oscillations of the pseudopotential inside r_c, already discussed in connection with Fig. 2. Fortunately, by employing the new optimized pseudopotential scheme described in Sec. II, we always generated very smooth optimized pseudopotentials. This allows us to construct $\Delta V_l(r)$ potentials which do not have strong-wavelength oscillations, and hence transform to KB form (3.1) without any difficulty.

It is important to ensure that the problem associated with "ghost states" can be controlled when using the KB form of pseudopotential. Gonze, Käckell, and Scheffler[11] have given a prescription for overcoming this problem, which has been used by Troullier and Martins[6] in constructing their soft pseudopotentials in KB form. We have also avoided, successfully so far, the problem of "ghost states" by following the same prescription.

Now we should consider the transferability of our optimized pseudopotential in KB form. There is no automatic way to predict or control transferability: one has to test any pseudopotential that has been generated, and if necessary modify it using one's general understanding of the factors that control transferability. When the potential is constructed, we only ensure that it will reproduce the all-electron calculation in the reference configuration. In practice, we want to use this potential in a wide range of atomic environments. To achieve this it is necessary for the potential to reproduce the all-electron results (a) for different valence electron densities on the atom and (b) over as wide a range of energies as possible for a fixed density. We can test this in two different directions. First the logarithmic derivative of the optimized KB pseudo-wave-function has been constructed and compared with that of the all-electron wave function. In Fig. 4, we have plotted the logarithmic derivatives of our 3*d* optimized and Kerker KB pseudo-wave-functions of Zn in comparison with that of the 3*d* all-electron wave function. As can be seen from Fig. 4, the scattering proper-

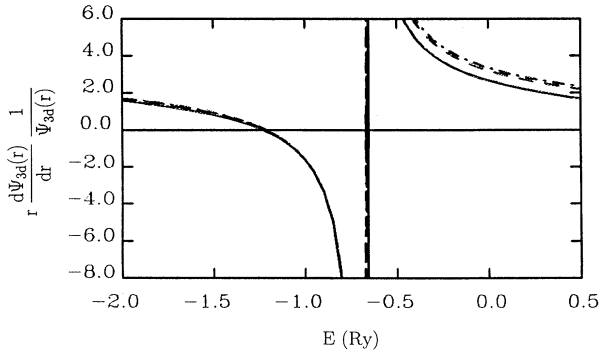

FIG. 4. The logarithmic derivatives of the all-electron radial wave function (solid line), Kerker (dashed line), and optimized (dash-dotted line) Kleinman-Bylander pseudo-wave-functions for 3*d* eigenstate of Zn with a core radius of 2.00 bohr. The atomic eigenvalue is −0.912 941 Ry.

ties of both the optimized and the Kerker KB form of the nonlocal pseudopotential are almost identical over a wide range of energies. Also, if we compare the curve of the KB form of the nonlocal optimized pseudopotential with that of all-electron potential, it can be seen that the transferability of the KB form of the nonlocal pseudopotential is still quite good given that the $3d$ electrons do not participate strongly in chemical bonding and will only be important over a small range of energies.

The all-electron logarithmic derivative at high energy is not reproduced as well as by the pseudopotential of Troullier and Martins. Nevertheless the deviation given by our potential is within the range of other pseudopotentials that have been tested and found satisfactory in solid-state applications. Pseudopotentials of several other atoms have been generated by the present scheme and tested by various groups in Britain.

However, the logarithmic derivative results are calculated with the assumption of constant screening by the valence electrons, and this is not the case when the environment of an atom changes in the solid. Therefore it is necessary to take a second step and test the KB form of the nonlocal optimized pseudopotential in a variety of atomic configurations. The principle is well established. The free-atomic configuration of Si is of course $3s^2 3p^2$, but in the diamond structure it is formally $3s 3p^3$, to give tetrahedrally directed valence orbitals in the usual way. Compression of the solid will also tend to promote electrons into higher $3p$ orbitals. In reality, the sp transfer x in the configuration $3s^{2-x}3p^{2+x}$ was found to vary between about $x=0.2$ and 0.6 over three different structures and a reasonable range of distances.[12] Thus one can mimic a change in solid-state environment by a change in atomic configuration. One generates a pseudopotential with one configuration, calculates with it a different configuration, and compares the energy eigenvalues of the second one with the corresponding all-electron calculation. Results of tests of this type of the KB form of the $3d$ nonlocal optimized pseudopotential and Kerker pseudopotential in different atomic configurations are presented in Table II. Both the semilocal form (2.3) and the KB form (3.1) of the optimized pseudopotentials yield almost the same eigenvalues as the all-electron calculations in all the atomic configurations. The difference in eigenvalues between the KB forms of the optimized and the Kerker pseudopotentials is almost negligible. When transferred to the different atomic configurations, the eigenvalues of the KB form of the optimized pseudopotential differ from those of the all-electron potential by only a small amount, quite small enough for normal physical applications.

IV. RESULTS FOR ZnS

We first investigated the total-energy convergence for cubic ZnS to verify that convergence occurred at the same energy as the atomic kinetic energy of the Zn pseudoatom. Since the $3d$ pseudopotential of Zn will control the total-energy convergence of cubic ZnS even after optimization, there is no need to optimize the $4s$ and $4p$ pseudopotentials of Zn or the $3s$, $3p$, and $3d$ pseudopotentials of S. We used the $3d$ optimized pseudopotential of Zn as described in Sec. II for this study. The $4s$ and $4p$ pseudopotentials for Zn were constructed using the $3d^{10}4s^{1.73}4p^{0.27}$ configuration and the Kerker scheme[9] with an r_c of 2.00 bohr. We also generated $3s$ and $3p$ Kerker pseudopotentials for S in the $3s^{1.86}3p^{4.14}$ configuration with core radii of 1.32 and 1.46 bohr, respectively, and a $3d$ Kerker pseudopotential for S in the $3s^{1.0}3p^{1.75}3d^{0.25}$ configuration with an r_c of 1.53 bohr. We then transformed these nonlocal pseudopotentials into KB form with s-wave and p-wave components treated as local for Zn and S, respectively. The pseudopotential total-energy calculations were carried out in the framework of the local-density approximation of density-functional theory using Perdew and Zunger's[13] parametrization of the exchange-correlation energy. The electronic minimization was performed using the conjugate gradient technique.[4] Two special Monkhorst-Pack[14] k points were used for Brillouin-zone sampling. Results for the total-energy convergence of cubic ZnS with a lattice parameter of 5.40 Å are shown in Table III. Indeed, the pseudopotential total energy of cubic ZnS was almost converged at a cutoff energy of 50 Ry, as we expected from the atomic kinetic-energy convergence of the pseudoatom of Zn. Increasing the cutoff energy up to 100 Ry decreased the total energy by only a further 0.07 eV. In comparison with recent results[15] for cubic ZnS using the soft pseudopotential of Troullier and Martins, in which the cutoff energy of 121 Ry had to be used, our optimized pseudopotential shows dramatically better convergence even though a smaller core radius was used. We then calculated the structural properties of cubic ZnS with a cutoff energy of 55 Ry by fitting the Murnaghan equation of state[16] to the calculated data points. Our results are compared with experimental values[17] in Table IV. The equilibrium lattice constant a_0, bulk modulus B_0, and its pressure derivative B_0' are in very good agreement with experiment. The overestimate of the cohesive energy E_c, which arises from the use of the local-density approximation, is expected.

It is not difficult to appreciate that the improvement in

TABLE II. Kohn-Sham eigenvalues using the all-electron potential (AE), the semilocal optimized pseudopotential (SOP), the Kleinman-Bylander form of the nonlocal optimized pseudopotential (KBOP), and the Kleinman-Bylander form of the nonlocal Kerker pseudopotential (KBKE) for the $3d$ eigenstate of Zn in different atomic configurations.

Configuration	AE (Ry)	SOP (Ry)	KBOP (Ry)	KBKE (Ry)
$4s^{1.27}4p^{0.73}3d^{10.00}$	−0.912 941	−0.912 950	−0.912 950	−0.912 950
$4s^{2.0}3d^{10.00}$	−0.797 336	−0.790 282	−0.790 290	−0.793 908
$4s^{1.0}3d^{10.00}$	−1.502 393	−1.508 101	−1.508 109	−1.503 128
$4s^{1.00}4p^{1.00}3d^{10.00}$	−0.951 247	−0.953 925	−0.953 926	−0.952 661

TABLE III. The calculated total energy for cubic ZnS per molecular unit at different cutoff energies for the plane-wave basis set.

Energy cutoff (Ry)	Total energy (eV)
30	−1667.1516
40	−1710.0554
50	−1713.4542
55	−1713.4942
60	−1713.5015
70	−1713.5137
80	−1713.5153
90	−1713.5204
100	−1713.5224

the convergence using our procedure is very sensitive to the r_c chosen for generating the pseudopotential. The larger the r_c we choose, the better the convergence we obtain. But the r_c for the pseudopotentials of first-row elements of the Periodic Table very often cannot be chosen to be very large. As a result, the improvement in the convergence for first-row elements, even using our new scheme, is not as good as that for transition metals. But our calculated results for MgO and diamond using optimized pseudopotentials for O and C with core radii of 1.50 and 1.60 bohr, respectively, show that the pseudopotential total energies for these systems still converge around 65 and 60 Ry, respectively. These results suggest that our optimized pseudopotentials give much faster convergence than both Kerker and HSC pseudopotentials. Nevertheless, there is some hope of systematically improving the convergence even further by using only three constraints, so that convergence is obtained at a cutoff energy of q_3^2 Ry rather than q_4^2 Ry. The generation of optimized pseudopotentials of first-row elements using this idea is presently in progress.

V. CONCLUSIONS

We have set out to generate the better atomic pseudopotential with respect to convergence while retaining good transferability and having computational efficiency. The optimized pseudopotential scheme of RRKJ has been modified into a more systematic procedure in order to construct truly optimized pseudopotentials as regards convergence and smoothness. There are three new features in this procedure. (i) The number of spherical Bessel functions needed to expand pseudo-wave-functions is restricted to being the same as the number of constraints applied to construct the optimized pseudopotential, namely, four. (ii) The cutoff q_c is chosen as q_4. (iii) The convergence for total-energy calculations with an expansion of plane waves will then be achieved at an energy of the order of q_4^2 Ry, no matter what r_c is chosen, where q_4 is itself proportional to r_c^{-1}. The KB form of the optimized nonlocal pseudopotential is employed to fulfill our requirement of computational efficiency in electronic-structure calculations. We have demonstrated the transferability of our optimized pseudopotential in KB form. Finally, the excellent and predictable pseudopotential total-energy convergence, as demonstrated by the calculated structural properties of cubic ZnS, will allow pseudopotential total-energy calculations with optimized and transferable nonlocal separable *ab initio* pseudopotential to be performed for a wide class of solid-state materials.

TABLE IV. Comparison of calculated structural properties of cubic ZnS and experimental values.

	Calculated	Experiment[a]
a_0 (Å)	5.379	5.4041
B_0 (GPa)	81.2	76.9
B_0'	5.1	4.91
E_c (eV)	7.67	6.33

[a]See Ref. 17.

ACKNOWLEDGMENTS

We wish to acknowledge the help of Dr. R. J. Needs through our use of Dr. S. Froyen's pseudopotential generation program and Dr. D. Bird's KB conversion program. One of us (J.S.L.) gratefully acknowledges discussions with Dr. N. Troullier on the KB form of pseudopotentials and Dr. A. M. Rappe, Dr. N. M. Harrison, and Dr. M. F. Chu on the optimization scheme. The work was supported financially by the Science and Engineering Research Council and the Natural Environment Research Council of the U.K.

*Present address: Davy Farady Laboratory, The Royal Institution, 21 Albemarle Street, London W1X 4BS, U.K.

†Present address: Centre of Theoretical and Applied Physics, Yarmouk University, Irbid, Jordan.

[1]P. Hohenberg and W. Kohn, Phys. Rev. **136**, B864 (1964); W. Kohn and L. J. Sham, *ibid.* **140**, A1133 (1965).

[2]W. E. Pickett, Comput. Phys. Rep. **9**, 115 (1989); S. Ihm, A. Zunger, and M. L. Cohen, J. Phys. C **12**, 4409 (1979).

[3]R. Car and M. Parrinello, Phys. Rev. Lett. **55**, 2471 (1985).

[4]M. P. Teter, M. C. Payne, and D. C. Allan, Phys. Rev. B **40**, 12 255 (1989).

[5]L. Kleinman and D. M. Bylander, Phys. Rev. Lett. **48**, 1425 (1982); D. C. Allen and M. P. Teter, *ibid.* **59**, 1136 (1987).

[6]N. Troullier and J. L. Martins, Phys. Rev. B **43**, 1993 (1991).

[7]K. Laasonen, R. Car, C. Lee, and D. Vanderbilt, Phys. Rev. B **43**, 6796 (1991); D. Vanderbilt, *ibid.* **41**, 7892 (1990).

[8]A. M. Rappe and J. D. Joannopoulos, in *Computer Simulation in Materials Science,* edited by M. Mayer and V. Pontikis (Kluwer, Dordrecht, 1991), pp. 409–422; A. M. Rappe, K. M. Rabe, E. Kaxiras, and J. D. Joannopoulos, Phys. Rev. B **41**, 1227 (1990).

[9]G. P. Kerker, J. Phys. C **13**, L189 (1980).

[10]D. R. Hamann, M. Schlüter, and C. Chang, Phys. Rev. Lett. **43**, 1494 (1979).

[11]X. Gonze, P. Käckell, and M. Scheffler, Phys. Rev. B **41**, 12 264 (1990).

[12]A. T. Paxton, A. P. Sutton, and C. M. M. Nex, J. Phys. C **20**, L263 (1987).
[13]J. P. Perdew and A. Zunger, Phys. Rev. B **23**, 5048 (1981).
[14]J. Monkhorst and J. D. Pack, Phys. Rev. B **13**, 5188 (1976).
[15]J. L. Martins, N. Troullier, and S. H. Wei, Phys. Rev. B **43**, 2213 (1991); N. Troullier and J. L. Martins, Solid State Commun. **74**, 613 (1990).
[16]F. D. Murnaghan, Proc. Natl. Acad. Sci. U.S.A. **30**, 244 (1944).
[17]*Physics of II-VI and I-VII Compounds, Semimagnetic Semiconductors,* edited by K.-H. Hellwege, Landolt-Börnstein, New Series, Group 3, Vol. 17, Pt. b (Springer-Verlag, Berlin, 1982), and references therein.